Optical and structural properties of TiO_2 films as a function of Nb doping concentration

G. Q. Wang · W. Lan · M. L. Yu · G. J. Han ·
Y. Wang · Q. Su · X. Q. Liu

Abstract $Ti_{1-x}Nb_xO_2$ ($x = 0$–0.06) films were prepared on quartz substrates by sol–gel spin coating and characterized by a variety techniques. The effect of Nb doping on the structural and optical properties of $Ti_{1-x}Nb_xO_2$ films were mainly investigated by X-Ray diffraction (XRD), Raman spectroscopy, Field-emission scanning electron microscopy and UV–vis transmittance spectroscopy. XRD and Raman study showed that the Nb doping inhibited the grain growth. The grain size decreased from 39.4 to 23.4 nm as the doping concentration increased from 0 to 0.06 in atomic percent. The UV–vis transmittance spectroscopy analysis revealed that the films exhibited 55–65% transmittance in the visible region and the band gap of films became wider with increasing Nb doping concentration.

1 Introduction

TiO_2 is an important commercial material in the early twentieth century, which is largely used as optical filter [1, 2], gas sensor [3], photo catalyst, dye sensitized solar cells [4] and coating materials [5]. One particular area of interest is used as coating materials in optical thin films because its high transmittance and high refractive index in the visible region with good chemical durability in hostile environments. TiO_2 crystallizes in three forms: anatase (tetragonal), rutile (tetragonal) and brookite (orthorhombic) [6]. Formation of a particular phase depends upon the nature of starting material, composition, doping element, preparation method and annealing temperatures. Rutile is found to be most stable phase. Anatase phase can form at temperature below 800 °C and transform into stable rutile phase at higher temperature [7]. Physical and chemical properties of the films obtained depend on films structure, composition and presence of impurities [8].

TiO_2 films have been prepared by various techniques such as electron beam evaporation [9], chemical vapor deposition [10], pulsed laser deposition [11], sputtering [12] and sol–gel process [13]. The generally used vacuum techniques are suitable for small area substrates. Films obtained by these methods are needed expensive equipment, and the films are non-stoichiometric and non-uniform. Contrary to vacuum techniques, sol–gel process is an industrially promising technique for preparation of thin films on large area substrates. It has several important advantages such as high purity, low cost, easy doping and the possibility of having a homogeneous mixture of two cations in the liquid state.

In this study we report the deposition of Nb-doped TiO_2 films on quartz substrates by spin-coating technique from precursor solution. We have studied the structural and optical properties of these films with different doping concentration.

G. Q. Wang · W. Lan
Key Laboratory for Magnetism and Magnetic Materials of Ministry of Education, Lanzhou University, 730000 Lanzhou, People's Republic of China
e-mail: wanggq04@lzu.cn

G. Q. Wang · W. Lan · M. L. Yu · G. J. Han · Y. Wang · Q. Su · X. Q. Liu (✉)
Department of Physics, School of Physical Science and Technology, Lanzhou University, 730000 Lanzhou, People's Republic of China
e-mail: xqliu@lzu.edu.cn

2 Experimental

TiO_2 sol was prepared from tetrabutyl titanate and Niobium (V) ethoxide in ethanol. Acetylacetone (acac) was

added as a chelating agent to decrease the reactivity and stabilize the sol. Acetic acid was added to initialize hydrolysis by esterification reaction with ethanol. In this case, molar ratio of composition of the pure TiO_2 sol was $1:0.3:0.2:34$ of $Ti(OC_4H_9)_4$/acac/acetic acid/ethanol. $Nb(OC_2H_5)_5$ was used as the precursor for Nb. The concentration of the metal ion was varied between $x = 0$ and $x = 0.06$, where x is the atomic percent of the metal ion defined as $x = [M/(M + Ti)]$. In each case, the Nb-doped sol was aged for 12 h before coating. TiO_2 films were prepared by spin-coating onto quartz substrates. Just after coating, the precursor films were dried at 100 °C for 10 min and then 400 °C for 10 min. Finally, dried gel films were annealed at temperatures 700 °C for 2 h in air.

The structure and morphology of the films were characterized by X-Ray powder diffraction (Rigaku RINT2400 with Cu Kα radiation), Micro-Raman spectrometer (Jobin-Yvon LabRAM HR800 UV, YGA 532 nm), and Field-emission scanning electron microscopy (Hitach, S-4800), respectively. Optical transmittance was carried out using a UV–visible spectrophotometer (Tu-1901) in the range of 300–800 nm. The thickness of the films was about 200 nm measured by Surface Profiler.

3 Results and discussion

X-Ray diffraction patterns for the films with varying dopant concentration annealed at 700 °C are depicted in Fig. 1. As shown, the peaks of anatase phase can only be observed. The experimental peak positions were compared with the standard JCPDS files (JCPDS 21-1272) and the corresponding miller indices were indexed. The grain size was evaluated using the full with at half maximum (FWHM) of the intense (1 0 1) diffraction peak of anatase TiO_2 according to the Scherer equation. The results are given in Fig. 2. Compared with those of pure TiO_2 films, for doped TiO_2 films average anatase grain sizes decreased. It is found that the introduction of Nb can be inhibited the anatase grain growth. In general terms, the grain growth hindering observed when our samples were doped with Nb was very similar to that found by other authors. The Nb^{5+} radius (0.70 Å) is slightly bigger than Ti^{4+} radius (0.68 Å) and this means that Nb^{5+} induces slight stress in TiO_2 lattice, which may hinder the growth of the TiO_2 crystallites, as was found by Sharma and Bhatnagar [14].

Figure 3 shows the Raman spectra of Nb-doped TiO_2 films with different doping concentrations. The spectra shows symmetric modes of vibration $A_{1g} + 2B_{1g} + 3E_g$ of tetragonal anatase phase identified at 141 (E_g), 200 (E_g), 397 (B_{1g}), 513 (A_{1g}), 519 (B_{1g}) and 637 cm^{-1} (E_g). The observed band positions are in agreement with the previous reports for anatase phase [15]. The Raman spectra of the
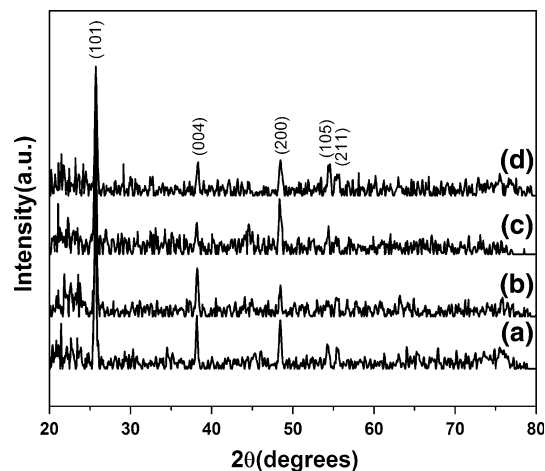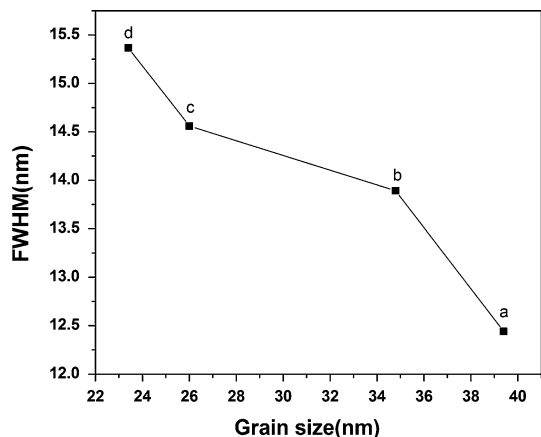

Fig. 1 X-ray diffractograms of Nb-doped TiO_2 films: (a) $x = 0$, (b) $x = 0.02$, (c) $x = 0.04$, (d) $x = 0.06$, where $x = Nb/[Nb + Ti]$
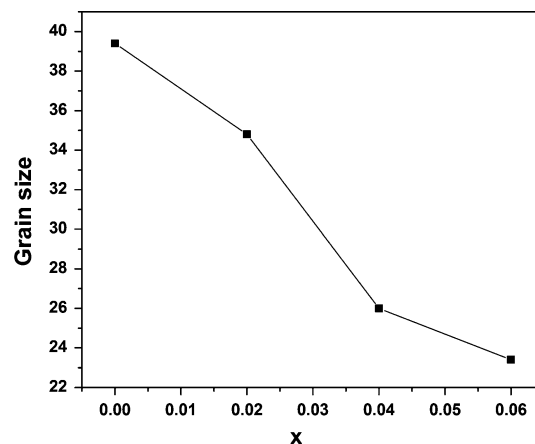
Fig. 2 The variation of grain size with different Nb-doped TiO_2 films
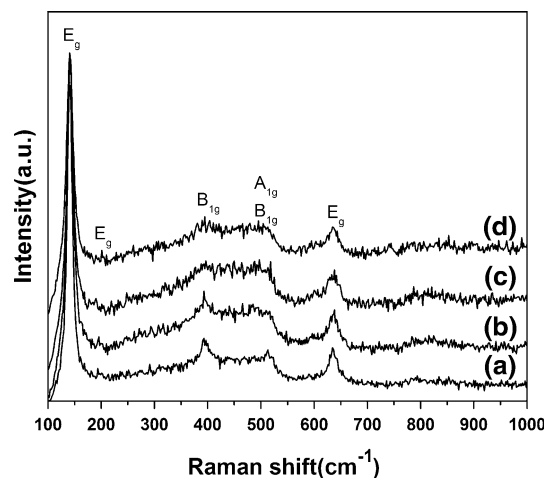
Fig. 3 Raman spectra of TiO_2 films with different Nb-doped concentration: (a) $x = 0$, (b) $x = 0.02$, (c) $x = 0.04$, (d) $x = 0.06$, where $x = Nb/[Nb + Ti]$
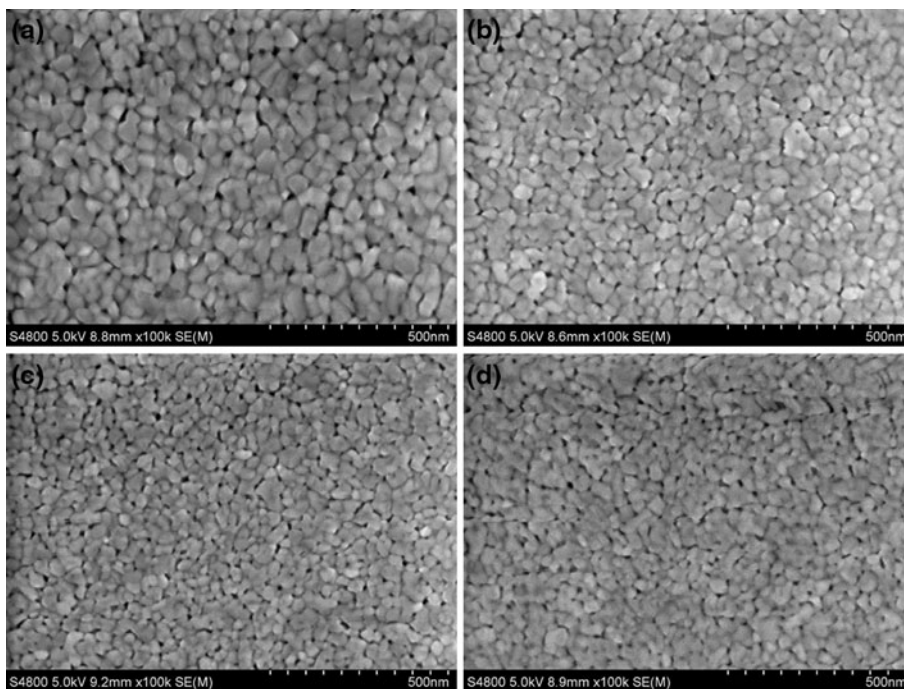
Fig. 4 Variation of FWHM of the Raman band at 144 cm^{-1} with grain size for the films with different doping concentration. ((a) $x = 0$, (b) $x = 0.02$, (c) $x = 0.04$, (d) $x = 0.06$, where $x = $ Nb/[Nb + Ti])

films doped with different doping concentration showed a broadening of the band with increasing doping concentration. However, no shift in peak position was observed. The FWHM of the main anatase peak (144 cm^{-1}) increased from 12.44 to 15.36 cm^{-1} as the doping concentration increased from 0 to 0.06 in atomic percent indicating a structural change, which has been shown in X-Ray studies. Figure 4 shows the variation of the FWHM of the Raman band (144 cm^{-1}) with grain size. It can be observed that the FWHM decreases following a first order exponential function which is given by equation:
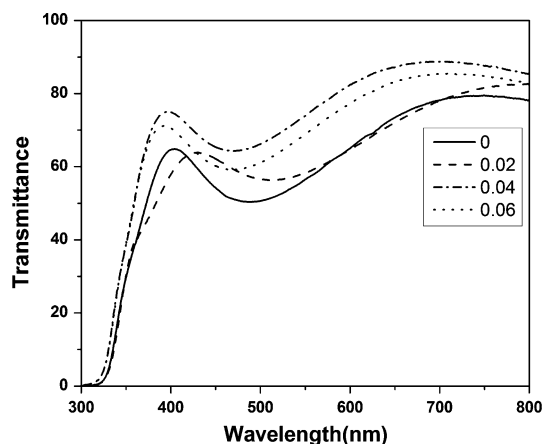
$$\text{FWHM} = A_1 e^{-(D-x_0)/t_1} + y_0$$

where D is the grain size in nm, $y_0 = 12.7468$, $x_0 = 16.6998$, $A_1 = 12.4878$, $t_1 = 0.2361$. This expression can be used to calculate the grain size from the Raman band. The results of Raman spectra show that the incorporation of different Nb concentration influenced the grain growth of the films, and those were similar to the XRD results.
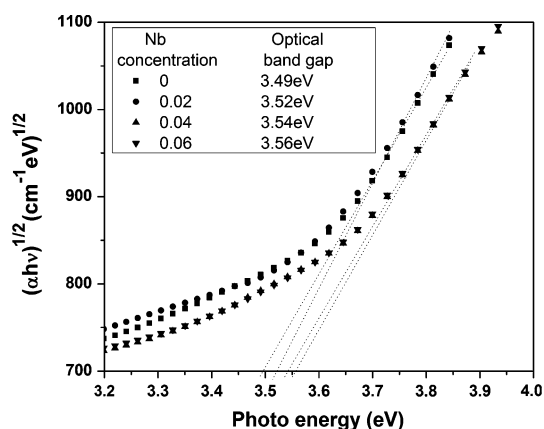
Figure 5 presents the SEM micrographs of TiO$_2$ films. All the films had similar microstructures. The surface of films was continuous, smooth and very uniform. The microphotographs confirm that sizes of anatase grains decreased with the Nb doping. SEM microphotographs show that the anatase grain sizes decreased from ca. 40 nm for pure TiO$_2$ films to ca. 20–25 nm for doped TiO$_2$ films, also. The result was similar to the XRD and Raman results.

In order to understand the effect of Nb doping on the optical properties of titanium dioxide films, optical transmittance was performed in the UV–visible region. Fig. 6 shows the transmission spectra of undoped and Nb-doped TiO$_2$ films in the wavelength range 300–800 nm. The wavy nature in the region 400–800 nm in transmission spectra was due to interference effect and a fast decrease in transmittance can be related to the excitonic transition [16]. All the films exhibit 55–65% transmittance in the visible region and start absorbing in between 350 and 400 nm. With increasing Nb concentration the absorption edge shifted towards lower wavelength side indicating the increase in the band gap of the films.

The optical band gap (E_g) of the films was calculated using the Tauc equation. The absorption coefficient (α) was

Fig. 5 SEM micrographs of Nb-doped TiO$_2$ films: **a** $x = 0$, **b** $x = 0.02$, **c** $x = 0.04$, **d** $x = 0.06$, where $x = $ Nb/[Nb + Ti]

Fig. 6 Transmission spectra of Nb-doped TiO_2 films

Fig. 7 $(\alpha h v)^{1/2}$ versus hv plots for Nb-doped TiO_2 films

estimated from the transmittance spectra using Newton-Raphson method. The band band gap was estimated by extrapolating the straight line portion of the $(\alpha h v)^{1/2}$ versus hv plot (as shown in Fig. 7). The band gap of the undoped film was 3.49 eV and it increased to 3.56 eV with increasing Nb concentration. The widening of the band gap can be explained by the Burstein-Moss (BM) effect [17], in which the lowest states in the conduction band were blocked, and transitions can take place only to energies higher than Fermi energy. Thus, the band gap became widening with increasing Nb doping concentration. The observes values were higher than the band gap of both bulk and thin film TiO_2 in the anatase phase. The reported values were 3.18 eV [18] for bulk material and in the range 3.2–3.23 eV for thin films [19]. The higher band gap observed in our case can be associated with the nano-crystalline nature of the films.

4 Conclusions

The effect of Nb doping (up to 0.06 in atomic percent) on the structural and optical properties of titanium dioxide films prepared by sol–gel spin coating technique has been examined. The surface of films was continuous, smooth and very uniform. All the films exhibit 55–65% transmittance in the visible region and start absorbing in between 350 and 400 nm. XRD and Raman study show that the Nb doping inhibited the anatase grain growth. The mechanism will be discussed in our later work.

References

1. R. Sun, A. Nakajima, I. Watanabe, T. Watanabe, K. Hashimoto, J. Photochem. Photobiol. A: Chem. **136**(1–2), 111–116 (2000)
2. W. Choi, J. Ko, H. Park, J. Chung, Appl. Catal. B: Environ. **31**(3), 209–220 (2001)
3. C. Garzella, E. Comini, E. Tempesti, C. Frigeri, G. Sberveglieri, Sens. Actuators: B. **68**(1–3), 189–196 (2000)
4. B. O'Regan, M. Gratzel, Nature. **353**(6346), 737–740 (1991)
5. B. Kear, Z. Kalman, R. Sadangi, G. Skandan, J. Colaizzi, W. Mayo, J. Thermal. Spray. Technol. **9**(4), 483–487 (2000)
6. F. Dachille, P. Simons, R. Roy, Am.Min. **53**, 1929–1939 (1968)
7. E.D. Palik, *Handbook of Optical Constants of Solids II* (Academic Press, New York, 1991), p. 795
8. C. Brinker, G. Scherer, *Sol-gel Science: the Physics and Chemistry of Sol-gel Processing* (Academic Press, San Diego, 1990), pp. 216–227
9. N. Rao, S. Mohan, J. Vac. Sci. Technol. A. **8**(4), 3260–3264 (1990)
10. E. Logothetis, W. Kaiser, Sens. Actuators. **4**, 333–340 (1983)
11. S. Yamamoto, T. Sumita, A. Miyashita, H. Naramoto, Thin. Solid. Films. **401**(1–2), 88–93 (2001)
12. M. Takeuchi, Thin. Solid. Films. **51**, 83–88 (1978)
13. T. Watanabe, S. Fukayama, M. Miyauchi, A. Fujishima, K. Hashimoto, J. Sol-Gel. Sci. Technol. **19**(1), 71–76 (2000)
14. R. Sharma, M. Bhatnagar, Sens. Actuators. B. **56**(3), 215–219 (1999)
15. T. Ohsaka, F. Izumi, Y. Fujiki, J. Raman. Spectrosc. **7**, 321–324 (1978)
16. S. Mahanty, S. Roy, S. Sen, J. Cryst. Growth. **261**(1), 77–81 (2004)
17. Y. Yang, X. Chen, Y. Feng, G. Yang, Nano. Lett. **7**(12), 3879–3883 (2007)
18. L. Hu, T. Yoko, H. Kozuka, S. Sakka, Thin. Solid. Films. **219**(1–2), 18–23 (1992)
19. Z. Wang, U. Helmersson, P.-O. Käll, Thin. Solid. Films. **405**(1–2), 50–54 (2002)